

# Ranking hand movements for myoelectric pattern recognition considering forearm muscle structure

Youngjin Na<sup>1</sup> · Sangjoon J. Kim<sup>1</sup> · Sungho Jo<sup>2</sup> · Jung Kim<sup>1</sup>

Received: 28 January 2016 / Accepted: 24 December 2016  
© International Federation for Medical and Biological Engineering 2017

**Abstract** Previous pattern recognition algorithms using surface electromyography (sEMG) have been developed for subsets of predefined hand movements without considering muscle structure. In order to decode hand movements, it is important to know which movements are appropriate for PR due to the different independence of movements between individuals and the high correlated characteristics of sEMG patterns between movements. This paper proposes a method to personally rank the order of hand movements from subsets (31 finger flexion, 31 finger extension, and 4 wrist movements in this paper). The movements were sorted into a ranked order with respect to the locations of the electrodes on the proximal forearm and the distal forearm. We evaluated the classification error as the number of desired movements ( $N_m$ ) changed. The maximum  $N_m$  with an error lower than 10% was 20 for the proximal forearm and 10 for the distal forearm from ranked movements of individuals. Our method could help to identify the optimized order of hand movements considering the personal characteristics of each individual.

**Keywords** Surface electromyography · Rank order · Pattern recognition · Hand movement

## 1 Introduction

Pattern recognition (PR) of surface electromyography (sEMG) has been studied for decoding the motion intent in human-machine interactions (e.g., powered prostheses, exoskeletons, and rehabilitation robots [26]). Dexterous movements have been decoded using different features and classification methods with high classification accuracy [4, 6, 8, 13, 16, 21, 25, 31–35, 37, 39]. To enhance the reliability of PR technique, several issues including electrode shift [38], variation in force [3, 17], variation in limb position [14], transient changes in EMG [5], and adherence to subset of admissible movements [27] were still studied.

Previously, a predefined subset of movements has been typically used for all subjects in PR studies, because accurate sEMG patterns could only be recorded under a strict experimental protocol [27]. However, the approach using normative movements is inadequate for hand movements which show subject-specific sEMG patterns and for amputees who need their own target movements [1, 23]. For hand movements, sEMG patterns show inter-task variability due to unique muscle structures of individuals [22]. The sEMG patterns of different movements could show similar patterns because the muscles responsible for the finger movements are located in the intermediate and deep layers of the forearm (cross talk) [29, 40]. In addition, independence of finger movements was varied according to individuals due to differences in anatomic factors including biomechanical connections between the digits and functional organization of multi-tendoned finger muscles [15].

Classification of finger movements has been performed for an optimal set of predefined finger movements without considering individual characteristics [2, 11, 20, 28, 36]. For example, Al-Timemy et al. [2] classified 15 finger movements, which are 12 individual finger movements

✉ Sungho Jo  
shjo@cs.kaist.ac.kr

✉ Jung Kim  
jungkim@kaist.ac.kr

<sup>1</sup> Department of Mechanical Engineering, Korea Advanced Institute of Science and Technology (KAIST), Daejeon, Republic of Korea

<sup>2</sup> School of Computing, Korea Advanced Institute of Science and Technology (KAIST), Daejeon, Republic of Korea

and three flexions of combined fingers for healthy subjects. They focused on increasing the classification accuracy and used the predefined finger movements for all subjects. The effects of subject-specific characteristics were not considered during the classification process. Analysis of the repeatability of a movement between trials and separability between movements within a trial could help to identify which movements are more appropriate for each subject. Kuiken et al. [7] used repeatability and separability indices to identify how sEMG patterns differ between novice and experienced groups. The repeatability refers to how well a movement can be performed consistently between trials: Performing some finger movements might be difficult to repeat for some individuals. The separability between movements refers to the distinctness of sEMG patterns compared with different movements. While the results showed that the repeatability between trials was comparable in two groups, the separability between movements was better in experienced groups. Both indices can be used for a quantitative analysis of sEMG patterns.

In this paper, we propose a method to rank the set of hand movements using processing sEMG patterns and to sort movements in the order of the easiness of classification for each individual. Unlike previous PR studies, a subset of movements was selected with a rank order prior to a classification process and then evaluated using PR algorithms as the number of desired movements ( $N_m$ ) changed. We instructed 20 healthy subjects to perform 66 hand movements as naturally as possible as though they perform the movements in everyday life. The 66 movements were 31 finger flexion movements, 31 finger extension movements, and 4 wrist movements. The 18 electrodes were used for the proximal forearm (11 electrodes) and the distal forearm (7 electrodes). The ranked order of movements was extracted for each location, respectively. We evaluated the classification errors for the ranked order and analyzed the effect of individuals and the electrode locations.

## 2 Materials and methods

The proposed method is outlined in Fig. 1. The experiment setup and experiment procedures are described in detail in Sects. 2.1 and 2.2. Signal processing for feature extraction and rank order extraction is reported in Sects. 2.3, 2.4 and 2.5. Classification is shown in Sect. 2.6.

### 2.1 Experimental setup

Eighteen bipolar electrodes sensors (DE-2.1 sensor; Delsys Inc., USA) were attached on the right proximal forearm and distal forearm for all subjects [19, 24]. Sensor specifications are  $41 \times 20 \times 5$  mm for case dimension and

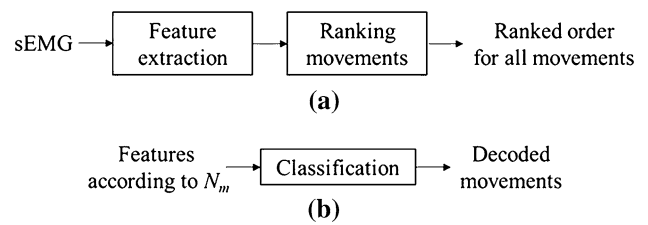


**Fig. 1** Schematic diagram for the proposed method **a** a ranking movement process and **b** a classification process using ranked order of movements. The protocol was repeated depending on the electrode locations and the subsets of movements from subject-specific and general order.  $N_m$  indicates the number of movements which is included for classification

$10 \times 1$  mm for contact electrode dimension. The signals were sampled at 1 kHz and were band-pass filtered using an FIR filter with a frequency range between 20 and 450 Hz [12, 18]. The electrodes were placed in two rows around the circumference of the thickest region of the upper proximal forearm (11 electrodes) and the distal forearm region proximally near the head of the ulna (7 electrodes) as shown in

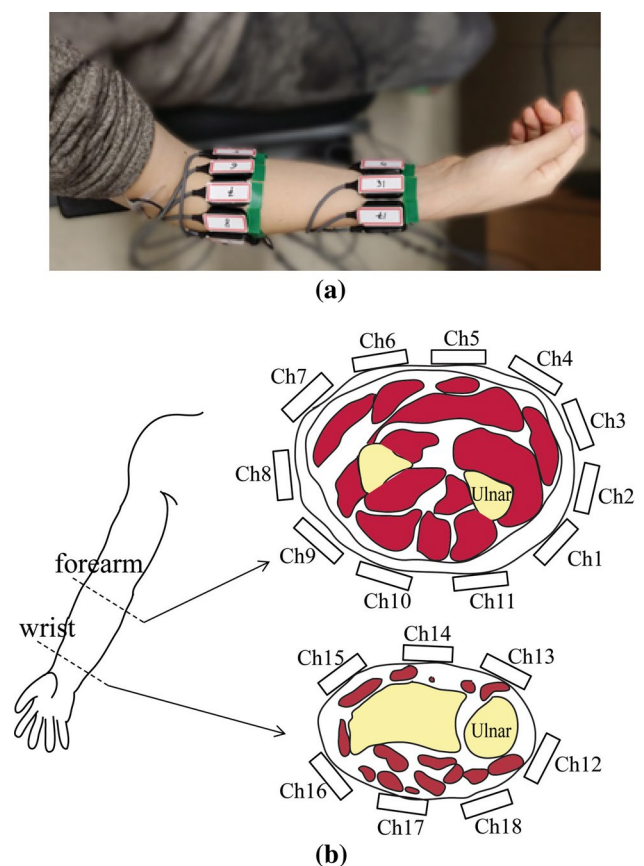


**Fig. 2** Experimental setup **a** top view of the right forearm and **b** 11 electrodes on the proximal forearm and 7 electrodes on the distal forearm

**Fig. 2.** The number of electrodes on the proximal and distal forearm was determined based on the subject with the thinnest circumference so that an equal number of electrodes can be applied for all subjects.

The circumferences were measured with a tapeline in order to determine attachment locations and the intervals between electrodes. Attachment locations were the thickness region on the forearm and the thinnest region proximally prior to the head of the ulnar. When electrodes were positioned, forearm was wrapped by a tapeline to attach electrodes with equidistant intervals. First electrodes for the proximal forearm and the distal forearm were determined next to the location of the ulnar bone (ch1 and ch12). Then each electrode was attached in the counter clockwise direction as shown in Fig. 2b. The ground reference electrodes were placed on the left wrist and on both elbow bones.

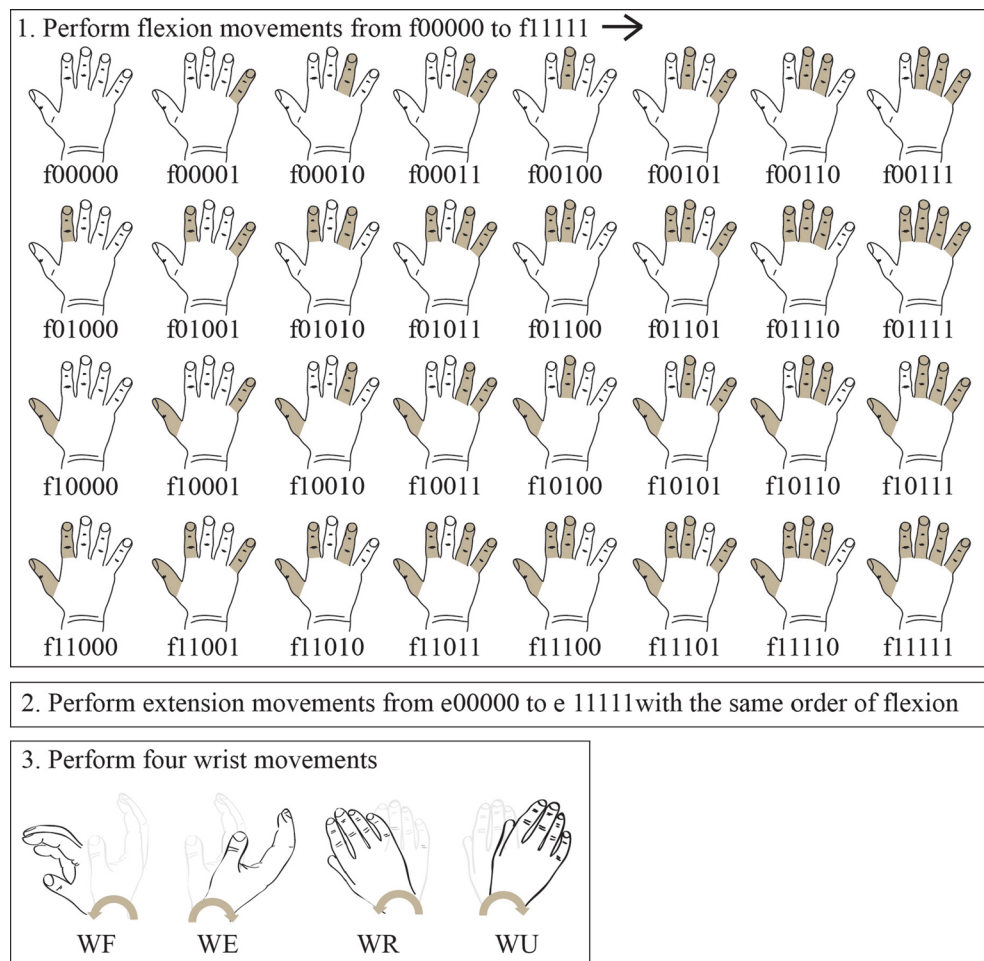
### 2.2 Experimental procedures

We recruited 20 healthy volunteers (14 males and 6 females,  $25.0 \pm 2.1$  years old,  $21.8 \pm 2.2$  body mass index, right-handed persons) who have no previous experience or

knowledge on pattern recognition experiments. The experimental protocol (KH2010-25) was approved by the Institutional Review Board at KAIST. Written informed consent and assent were obtained from the subjects. The subjects were asked to sit comfortably on a chair and to place their right elbow on the chair’s armrest. The subjects placed their hand so that the thumb pointed upwards and the little finger pointed downwards, as if handshaking (see Fig. 2a). The subjects maintained a rest posture (no movement), which is defined as the posture when the amplitudes of all sEMG signals were lower than a threshold.

We asked the subjects to perform 62 finger movements and 4 wrist movements as shown in Fig. 3. Each finger has three possible states: flexion, extension, and rest. Thirty-one allowable flexion movements were performed, and then, the 31 extension movements were carried out in the same manner. After performing all finger movements, the 4 wrist movements of wrist flexion, extension, radial deviation, and ulna deviation were performed. During whole processes, an experimenter checked whether or not a subject performed each movement according to a visual guide. If a subject made a mistake for some movements,

**Fig. 3** Sixty-six movements were used in this study. The order of flexion movements increased with one from the little finger as a binary number. The extension movements are performed in the same order, and then, the 4 wrist movements are performed. “I” indicates the flexion/extension, and “O” indicates the rest of each finger. WF, WE, WR, and WU were wrist flexion, extension, radial deviation, and ulna deviation



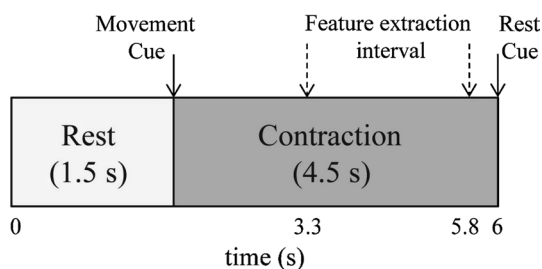


**Fig. 4** A movement is performed for 6 s with a 1.5 s rest and 4.5 s contraction. After the movement cue by the visual, the subject performs the movement until the rest cue is given and then the next movement is performed [36]

corresponding movements were performed again and then a single trial was finished. Prior to experiments, subjects were familiarized with a visual interface and performed each movement following a visual guide.

There were several movements that were uncomfortable or challenging to perform for some of the subjects because of the muscle anatomy of the human hand. We asked the subjects to perform the movements as naturally as possible. “Naturally” means that it is acceptable to move other fingers if the subject cannot move the instructed finger independently. The subjects were instructed to apply force only

to the designated finger, while trying to relax the fingers that are coupled with the instructed finger.

Subjects performed 10 trials. They produced movements with a moderate force. To avoid muscular and mental fatigue, they had 2 min of rest time after each trial. Subjects were asked to perform each movement for 4.5 s followed by 1.5 s of rest for all 66 movements continuously during a single trial, as shown in Fig. 4.

### 2.3 Feature extraction

The time-domain features were extracted every 50 ms during the time interval between 3.3 and 5.8 s of each movement with a time window of 200 ms in duration [36]. This time region was selected considering the delay between the movement cue and actual finger movements and the movements in advance of the rest cue. A sample sEMG data set during f11111 (S01) is represented in Fig. 5. Features were normalized with maximum values from each channel on each trial. The four time-domain features, the mean absolute value (MAV), waveform length (WL), zero crossing (ZC), and slope sign change (SSC), were calculated [26] (see “Appendix” for the detail). The characteristics of MAV and WL are strongly correlated, and the characteristics of ZC and SSC are also correlated [9]. The ZC and SSC

**Fig. 5** Raw sEMG data during f11111 movements (S01, ch01–ch11 for the proximal forearm and ch12–ch18 for the distal forearm). The signals prior to 1.5 s were generated by previous movements f11110 because all movements were continuously performed from f00001 to WU. The solid line at 1.5 s indicates the movements cue, and the dashed line from 3.3 to 5.8 s represents the extraction region for feature extraction and classification

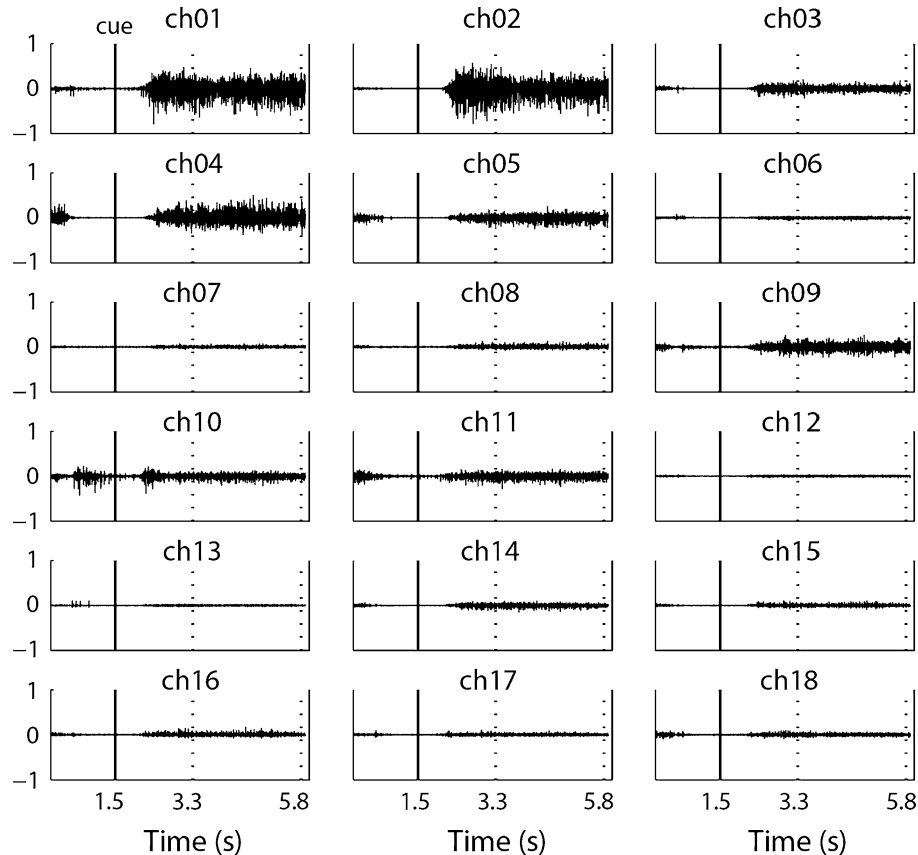


exhibit give indications of how quickly the signal changes. The features were extracted for the proximal forearm with 11 electrodes and the distal forearm with 7 electrodes, respectively.

## 2.4 Analysis for ranking movements

In ranking process, candidate movements were sorted based on the distance within a movement and between movements. The Bhattacharyya distance (BD) has been widely used as a class separability measure for feature selection. The BD was used to quantitatively analyze how well classes were separated and each class was well distributed. The BD is contained two information for repeatability within a class and separability between classes to assess the feature distributions of two classes. For two classes, the BD is calculated as follows [10].

$$BD_{ij} = \frac{1}{8}(\mu_1 - \mu_2)^T \left[ \frac{\sum_1 + \sum_2}{2} \right]^{-1} \times (\mu_1 - \mu_2) + \frac{1}{2} \ln \frac{|(\sum_1 + \sum_2)/2|}{|\sum_1|^{1/2} |\sum_2|^{1/2}}, \quad (1)$$

where  $\mu_i$  and  $\sum_i$  are the mean vector and covariance matrix of class  $i$ , respectively. In general, features of movements are well separated and classified as the BD is larger.

In data set composed of several classes, we assumed that the minimum of the BD value between two movements would indicate that how well features of movements were distributed without regard to that of other movements which have larger BD. Indeed, the minimum of the BD highly influences on classification error. The rank of movements was determined using the algorithm represented in Table 1. Set  $G$  is the set of ordered movements and is initially empty. Set  $R$  is the set of remaining movements from 1st to 68th initially including all movements. When all movements were included in set  $G$  and removed from set  $R$ , the algorithm was finished. The result of the algorithm was the ordered movements in  $G$ .

To avoid biased classification results when all trials were included in calculating the rank, five odd-numbered trials among 10 trials were used and the remaining five even-numbered trials were excluded for calculating the rank.

## 2.5 Subject-specific and general ranked movements

The optimal rank order of movements was independently selected for each individual using the algorithm in Sect. 2.4. The ranked order of each individual is “personalized.” In order to compare the classification performance between the personalized rank order for each individual and a generalized rank order, the generalized rank order was extracted based on the rank orders of 20 individuals. The sum of rank

order for each movement was sorted as descending order. The movement with the smaller sum of rank order implies that the movement has a higher rank. Therefore, the movements with higher rank were consecutively set as the generalized rank order. The above processes were performed for the proximal forearm and the distal forearm, respectively.

## 2.6 Classification

For classification process, the five odd-numbered trials were used for the training set in order to optimize model parameters and the five even-numbered trials were used for the test set among 10 trials for each subject [2]. Linear discriminant analysis (LDA) classifier was selected over other methods for classification because LDA can be simply implemented and fast optimized for training and test process [23].

The sorted movements in set  $G$  from Sect. 2.4 were evaluated based on the classification error because we cannot guarantee how well the selected movements were classified. The  $N_m$  for classification increased based on a selected rank order. For example, if the  $N_m$  was 15, the 1st to 15th movements in set  $G$  were used in the classification process.

## 3 Results

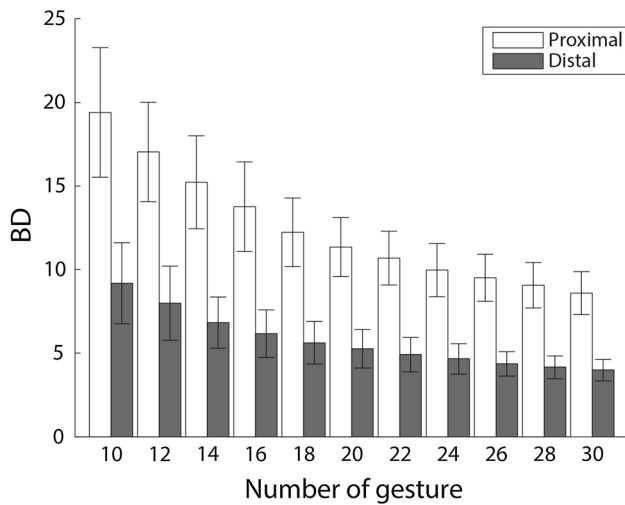
Figure 6 shows the average BD according to the  $N_m$  from 10 to 30 for the proximal and the distal forearms. The BD decreased as the  $N_m$  increased. The higher BD, calculated by Eq. (1), indicated that the sEMG features were distributed for better clustering. At each  $N_m$ , the BD showed statistical significance ( $p < 0.05$ ) between the proximal and the distal forearms. For each condition ( $N_m$  and electrode location), sample size was 20 because five odd-numbered trials were used to calculate a single value of the BD for 20 subjects. Statically analysis was performed using the Mann–Whitney test.

Figure 7 shows the average classification errors using LDA according to the  $N_m$  from 10 to 30 for the proximal and the distal forearms. As the  $N_m$  increased, the classification errors increased for both conditions. The maximum  $N_m$  with an error lower than 10% was 20 for the proximal and 12 for the distal. At each  $N_m$ , the classification error showed statistically significant difference ( $p < 0.05$ ) between the proximal and the distal forearms except 18, 20, and 22  $N_m$ . The component of selected movements was different for individuals because the optimal movements were selected by the rank analysis for each subject (subject-specific condition). For all classification results, sample size was 100 because five even-numbered trials were used for 20 subjects. Statically analysis was performed using the two-sample  $t$  test.

**Table 1** Algorithm for ranking movements using the Bhattacharyya distance (BD)

**Data:** features of each movement,  $M$   
**Results:** ranked movement set,  $G$   
**Initialize:**  
 $G = \{ \}$   
 $R = \{M_1, M_2, \dots, M_{68}\}$ , candidate set  
 $C = \{(M_1, M_2), (M_1, M_3), \dots, (M_{67}, M_{68})\}$ , all pairs of movements in  $R$   
 Find the pair with the maximum BD from  $C$   
 $G = \{M_i, M_j\}$   
 $R = R \setminus \{M_i, M_j\}$   
**while** length( $R$ ) > 0 **do**  
   **for**  $i = 1$ : length( $R$ ) **do**  
      $C_i$ , all pairs of the union composed of all movements in  $G$  and the  $i$ th movement in  $R$   
     **Find minimum BD<sub>*i*</sub>** from the computed BDs using pairs in  $C_i$   
   **end**  
   **Find the *i*th movement** which has the maximum BD  
    $G = G \cup M_i, R = R \setminus M_i$

'\setminus' indicates a relative complement



**Fig. 6** Average BD obtained from the proximal and the distal forearm for 10–30  $N_m$

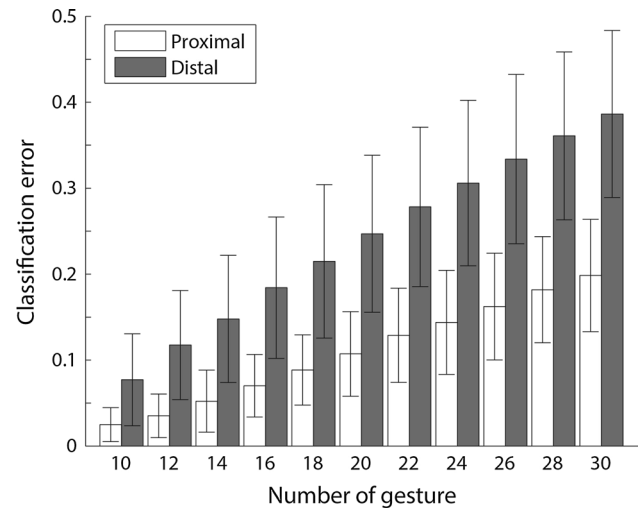


**Fig. 7** Average classification errors obtained from the proximal and the distal forearm for 10–30  $N_m$

Figure 8 shows the average classification error of a subject-specific set and a general set using LDA for the proximal and the distal forearm locations. As the  $N_m$  increased, the classification errors increased in both locations. The classification errors showed statistically significant difference ( $p < 0.05$ ) between the specific and the general from 12 to 30 for the proximal. For the distal, no significant differences ( $p < 0.05$ ) were shown for all  $N_m$ . Other conditions showed no difference between the specific and the general for both locations. Depending on the electrode locations, different generalized movements were extracted as shown in Table 2. All wrist movements and rest were included

within 1st to 5th order in both locations. Twenty-four movements marked in bold font in Table 1 were included within the 30th movements for both locations.

Figure 9 shows the relationship between the classification error and the BD for the proximal forearm and the distal forearm. Each of the data was obtained when the  $N_m$  was changed from 10 to 30 and the components of movements were the optimal movements for each subject. Exponential functions were chosen to fit.  $R^2$  were 0.54 for the proximal and 0.58 for the distal. In order to acquire the classification error less than 10% without regard to the  $N_m$ , BD has to be greater than 11.35 for the proximal and 7.88 for the distal.

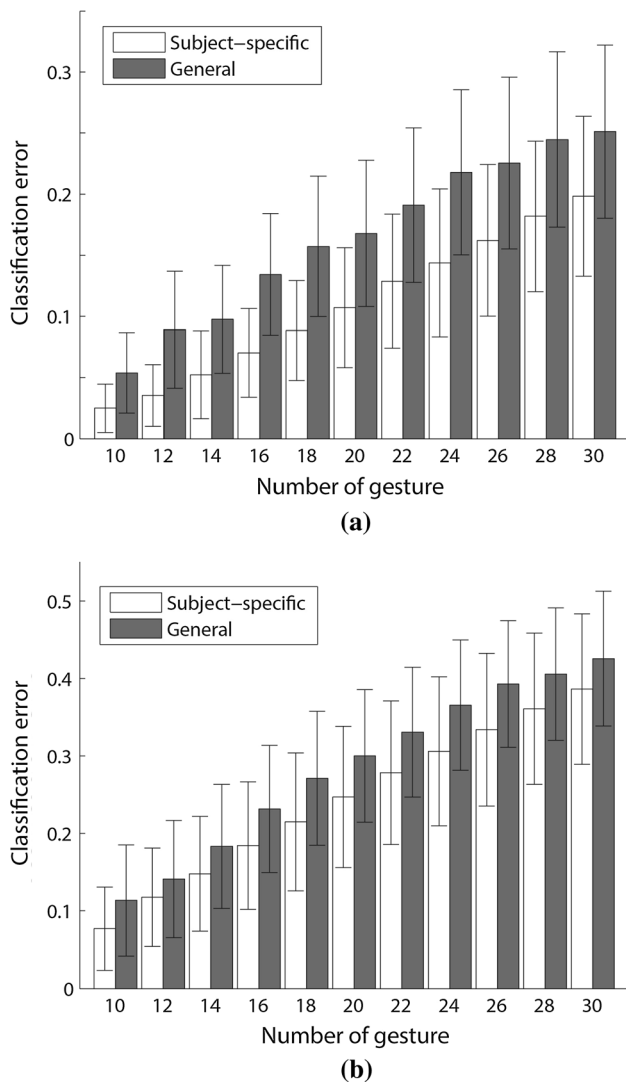


**Fig. 8** Average classification errors obtained from the specific and the general ranked movements for **a** the proximal and **b** the distal forearm

## 4 Discussion

In this study, we proposed the strategy to sort the movements as a rank order. In order to quantitatively determine the rank order of movements, the BD was calculated using sEMG features as the  $N_m$  increased. As a result, the ranked movements were extracted using the BD as shown in Table 2. Compared with previous pattern recognition studies, our method can help to choose the movements that can be used and to select movements that are wanted by a subject in prior to classification.

The candidate movements were 62 allowable finger movements and 4 wrist movements as shown in Fig. 3. We thought that repeatability of 66 movements was more

important because it is difficult to maintain a consistent contraction for each movement if a sequence order was randomly selected. The allowable finger movements included flexions from rest and extensions from rest. The combinations composed of flexion and extension (e.g., thumb and index flexion and other fingers extension) were neglected because these movements were awkward in a daily life. Instead, the 4 wrist movements were added for the candidate movements because wrist movements were widely used to classify in previous studies. The wrist flexion/extension and radial/ulnar deviation were used in this study. Compared with finger movements, the wrist movements were selected as the higher order in ranked movements as shown in Table 2 because sEMG patterns during wrist movements show more distinct features than finger movements. The muscles related to wrist movements are located in the superficial layer, and relationship between muscles and movements represents independent relationship rather than finger movements.

Previous studies reported that each finger movement was performed with other fingers movements and that the dependency of the coupling movement differed for each finger [15, 22]. The movements of the thumb and index finger were more highly individualized than the movements of the middle, ring, and little fingers [15]. Independence is determined by separation of tendons for each finger in the muscle mechanical structure [22]. The effect of their muscle structure could be different for individuals. However, in classification studies, there was no attempt to consider the muscle structure effects on finger movements. The proposed method provided not only the specific ranking movements for each individual, but also the generalized ranking movements that were applied for all subjects. The generalized movements were selected for the proximal and the distal forearms (Table 2).

The classification of finger movements is more challenging compared with other movements because recorded sEMG signals on forearms show low amplitude and not distinct characteristics. As mentioned, muscles which relate to finger movements were located in the intermediate and deep layers of the forearm. Figure 10 shows that why the classification of finger movements is more difficult using raw sEMG data. The raw sEMG was recorded on the proximal forearm for S01 and S19 during two finger movements (f00111 and f10111). The sEMG characteristics showed similar patterns for different finger movements in a same subject, and the same movement showed the different amplitudes according to subjects. The amplitudes of S01 (left figure) were larger than those of S19 (right figure). Therefore, we proposed the method to extract the ranked movements. This approach not only removed unreliable movements, but also extracted optimal movements for individuals.

**Table 2** Generalized ranked movements among 31 flexions and 31 extensions finger movements and 4 wrist movements

Rank order	Electrode location		Rank order	Electrode location	
	Proximal	Distal		Proximal	Distal
1	<b>Rest</b>	<b>Rest</b>	16	<b>F10000</b>	<b>F01000</b>
2	<b>WE</b>	<b>WU</b>	17	<b>E11000</b>	<b>F01111</b>
3	<b>WF</b>	<b>WE</b>	18	F10010	<b>F11110</b>
4	<b>WR</b>	<b>WF</b>	19	<b>F00100</b>	F01001
5	<b>WU</b>	<b>WR</b>	20	<b>E00100</b>	<b>F00011</b>
6	<b>F11111</b>	<b>F11111</b>	21	<b>F00011</b>	<b>E10001</b>
7	<b>E10001</b>	<b>F00001</b>	22	<b>F00110</b>	<b>F00111</b>
8	<b>E01000</b>	<b>E10000</b>	23	<b>F10111</b>	F10011
9	<b>F00001</b>	<b>E01000</b>	24	<b>F11011</b>	F11000
10	<b>F00111</b>	<b>E00001</b>	25	<b>F11110</b>	F10111
11	<b>E00001</b>	<b>F10000</b>	26	E10111	<b>F10111</b>
12	<b>E10000</b>	<b>F00010</b>	27	F11100	<b>F00110</b>
13	<b>F00010</b>	<b>F00100</b>	28	F01010	E11101
14	<b>F01000</b>	<b>E00100</b>	29	F11001	<b>F10111</b>
15	<b>F01111</b>	F10001	30	E11100	<b>F00100</b>

Movements with bold are included in both locations

For classification of finger movements, previous studies have investigated finger flexion and extension movements with single finger only and have not thoroughly addressed combinations of fingers. They have used a subset of predefined movements for all subjects. Al-Timemy et al. [2] classified three multi-finger movements and 12 single-finger movements. Tenore et al. [36] used the extension and flexion of the middle, ring, and little fingers and 10 single-finger movements. Cipriani et al. [11] analyzed four multi-finger movements as grip types (e.g., tridigital grip and lateral grip) and three single-finger movements. We classified the ranked movements as the  $N_m$  changed. Figure 8 shows the classification error of the specific and the general ranked movements for the proximal and the distal forearms. Although the classification error increased as the  $N_m$  increased, our method achieved less than 10% error with the 20 movements for the proximal and 12 movements for the distal.

The classification error was used to evaluate the efficacy of proposed method. An artificial neural network (ANN) was also used to compare the classification performance with LDA. For ANN, the number of hidden-layer neurons was equal to the mean of the dimensions in the input and output. The input dimension was determined using the number of electrodes and features. The dimension of the output neurons was varied depending on the  $N_m$ . High activation of the output neurons indicates that the ANN optimizes the corresponding class as its best guess. There were no significant differences between ANN and LDA for all

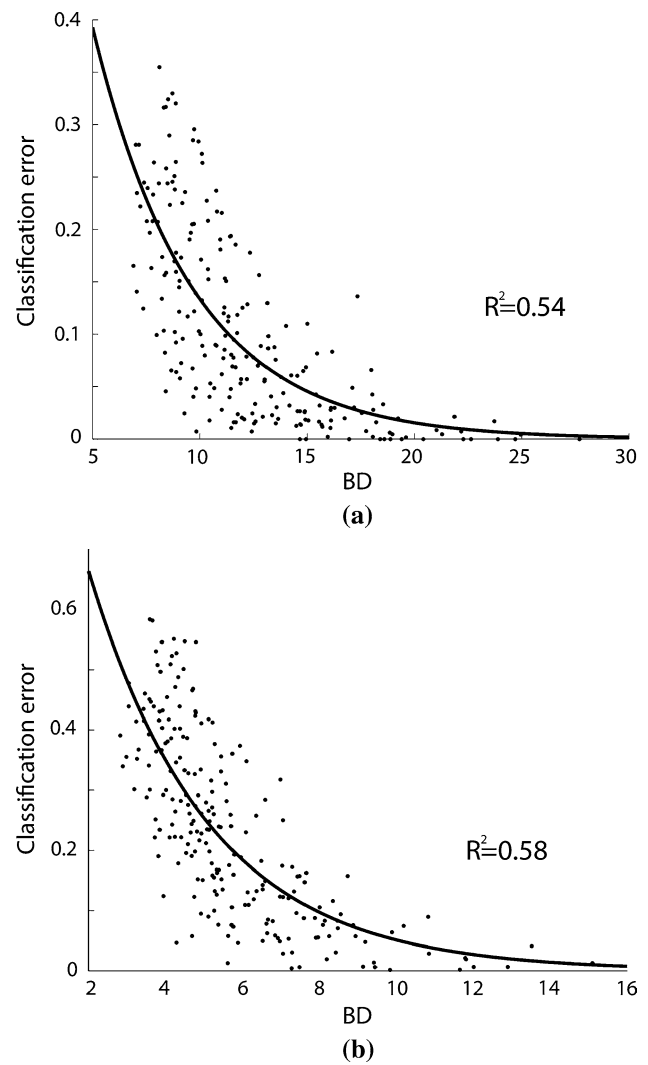


**Fig. 9** Exponential fits of the BD to classification errors for **a** the proximal forearm and **b** the distal forearm

conditions. We did not compare the performance with other methods because the improvement of the classification error with classification algorithms was beyond the scope of this study. The classification error could be improved using the previously reported classification techniques, although the  $N_m$  differed in accordance with the experimental conditions. The trend of classification might be similar that the  $N_m$  increased the classification error increased regardless of a classification technique.

The effect of electrode location on the BD and the classification error was investigated for the extrinsic muscles on the forearm. The muscles located on the forearm have been widely used because the number of available sites is limited for intrinsic muscles. In this study, locations were divided for the proximal forearm and the distal forearm as shown in Fig. 2. The extracted generalized movements showed similar components for the rest

and 4 wrist movements that were contained within 5th order for both locations as shown in Table 2. The same 24 movements were included for both locations among 30 movements from 1st to 30th. Compared with the distal forearm, proximal forearm showed superior results (classification errors) although the components of movements were different.

Previous PR studies have used many electrodes on the forearm for wrist and finger movements classification. Depending on subject condition and experimental setup, locations of electrodes were changed. Although this approach provides more accurate classification results, the increase in electrode number showed limited improvement in terms of accuracy after certain number of electrodes. Several studies were performed to determine the optimal number of electrodes in PR. Al-Timemy et al. [2] showed that the classification accuracy for 15 finger movements reached a plateau using 6 electrodes despite the use of a total of 12 electrodes on the forearm. Naik et al. [30] proposed a method to determine the minimum number of electrodes based on independent component analysis (ICA) and

Icasso clustering for 12 finger movements. Fewer number of electrodes would provide dexterity, flexibility, and controllability for PR-based systems. However, in this study, same number of electrodes was used 11 electrodes for the proximal forearm and 7 electrodes for distal forearm to maintain consistent experimental setup for all participants. In other words, we did not consider finding the optimal number of electrode in this study.

The proposed method could be used for sEMG-based interfaces in a normal use scenario. First, usable movements could be extracted from all allowable movements. The ranked movements and corresponding accuracy could be provided depending on the number of input commands as the user desires. The BD value might be an indicator to determine whether which movements are included or not. Second, if a user desires specific movements for input commands, the availability of the desired movements could be evaluated based on the BD. The desired movements are not recommended if the movements exhibit inconsistent sEMG features, but the movements are selected for input commands if the movements have reliable and repeatable characteristics.

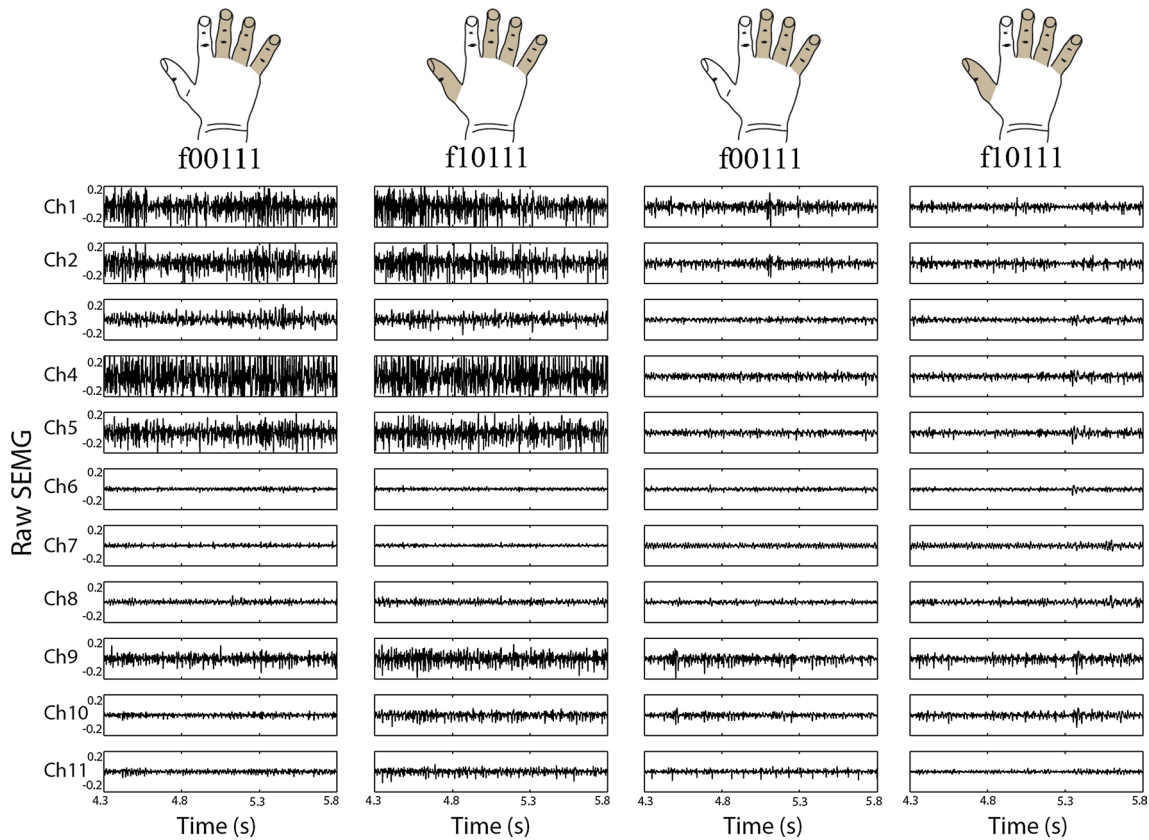


**Fig. 10** Raw sEMGs of Ch1 to Ch11 on the proximal forearm. **a** f00111 and **b** f10111 for S01; **c** f00111 and **d** f10111 for S19. The f00111 is the middle, ring, and little finger flexion. The f10111 flexion is the thumb, middle, ring, and little finger flexion

## 5 Conclusion

We investigated a ranking method to extract appropriate hand movements among candidate movements using sEMG patterns in prior to a classification process. Our method provided the ranked movements from 62 finger movements and 4 wrist movements using the BD values that are criteria to identify whether a subset of movements was approximately clustered for classification. The subject-specific and general ranked movements were extracted from the proximal forearm and distal forearm. For the subject-specific condition, the maximum  $N_m$  with an error lower than 10% was 20 for the proximal forearm and 12 for the distal forearm. For the general condition, classification errors were greater than that of the subject-specific condition. Using the proposed method that considers their personal characteristics, user could create more commands with their movements for PR techniques.

**Acknowledgements** This research was supported by the National Research Foundation of Korea (NRF) grant funded by the Korea government (MBDP) (No. 2015-002966). This work was supported by Basic Science Research Program through the National Research Foundation of Korea funded by the Ministry of Education (2013R1A1A2009378).

## Appendix

Mathematical definitions of time-domain features which were used in this study are as follows [26].  $x_i(k)$  is the  $k$ th signal sample,  $i$  is the  $i$ th window,  $N$  is the number of samples in the window, and  $xth$  is the threshold value.

### Mean absolute value (MAV)

$$MAV_i = \frac{1}{N} \sum_{k=1}^N |x_i(k)|, \quad (2)$$

### Waveform length (WL)

$$WL_i = \sum_{k=1}^{N-1} (|x_i(k) - x_i(k+1)|). \quad (3)$$

WL is a combined measure of waveform amplitude, frequency, and duration.

### Zero crossing (ZC)

$$ZC_i = \sum_{k=1}^N f(k), \quad (4)$$

where

$$f(x) = \begin{cases} 1, & \text{if } x_i(k) \times x_i(k+1) < 0 \text{ and } |x_i(k) - x_i(k+1)| > xth \\ 0, & \text{otherwise.} \end{cases}$$

ZC represents the number of points in the window where the sign of a function changes (e.g., from positive to negative). This feature is an estimate of the properties in the frequency domain.

### Slope sign change (SSC)

$$SSC_i = \sum_{k=2}^{N-1} f[(x_i(k) - x_i(k-1)) \times (x_i(k) - x_i(k+1))], \quad (5)$$

where

$$f(x) = \begin{cases} 1, & \text{if } x > xth \\ 0, & \text{otherwise.} \end{cases}$$

This feature is similar to ZC regarding the frequency properties.

## References

1. Al-Timemy AH, Escudero J, Bugmann G, Outram N (2013) Protocol for site selection and movement assessment for the myoelectric control of a multi-functional upper-limb prosthesis. *Annu Int Conf IEEE Eng Med Biol Soc* 2013:5817–5820
2. Al-Timemy AH, Bugmann G, Escudero J, Outram N (2013) Classification of finger movements for the dexterous hand prosthesis control with surface electromyography. *IEEE J Biomed Health Inform* 17(3):608–618
3. Al-Timemy A, Khushaba R, Bugmann G, Escudero J (2015) Improving the performance against force variation of EMG controlled multifunctional upper-limb prostheses for transradial amputees. *IEEE Trans Neural Syst Rehabil Eng* 24(6):650–651
4. Amsüss S, Goebel PM, Jiang N, Graitmann B, Paredes L, Farina D (2014) Self-correcting pattern recognition system of surface EMG signals for upper limb prosthesis control. *IEEE Trans Biomed Eng* 61(4):1167–1176
5. Artemiadis PK, Kyriakopoulos KJ (2010) An EMG-based robot control scheme robust to time-varying EMG signal features. *IEEE Trans Inf Technol Biomed* 14(3):582–588
6. Artemiadis PK, Kyriakopoulos KJ (2011) A switching regime model for the EMG-based control of a robot arm. *IEEE Trans Syst Man Cybern Part B Cybern* 41(1):53–63
7. Bunderson NE, Kuiken TA (2012) Quantification of feature space changes with experience during electromyogram pattern recognition control. *IEEE Trans Neural Syst Rehabil Eng* 20(3):239–246

8. Cesqui B, Tropea P, Micera S, Krebs HI (2013) EMG-based pattern recognition approach in post stroke robot-aided rehabilitation: a feasibility study. *J Neuroeng Rehabil* 10:75
9. Chattopadhyay R, Jesunathadas M, Poston B, Santello M, Ye J, Panchanathan S (2012) A subject-independent method for automatically grading electromyographic features during a fatiguing contraction. *IEEE Trans Biomed Eng* 59(6):1749–1757
10. Choi E, Lee C (2003) Feature extraction based on the Bhattacharyya distance. *Pattern Recognit* 36(8):1703–1709
11. Cipriani C, Antfolk C, Controzzi M, Lundborg G, Rosen B, Carrozza MC, Sebelius F (2011) Online myoelectric control of a dexterous hand prosthesis by transradial amputees. *IEEE Trans Neural Syst Rehabil Eng* 19(3):260–270
12. De Luca CJ, Gilmore LD, Kuznetsov M, Roy SH (2010) Filtering the surface EMG signal: movement artifact and baseline noise contamination. *J Biomech* 43(8):1573–1579
13. Ertuğrul ÖF, Kaya Y, Tekin R (2015) A novel approach for SEMG signal classification with adaptive local binary patterns. *Med Biol Eng Comput* 54(7):1137–1146
14. Fougner A, Scheme E, Chan ADC, Englehart K, Stavadahl Ø (2011) Resolving the limb position effect in myoelectric pattern recognition. *IEEE Trans Neural Syst Rehabil Eng* 19(6):644–651
15. Häger-Ross C, Schieber MH (2000) Quantifying the independence of human finger movements: comparisons of digits, hands, and movement frequencies. *J Neurosci* 20(22):8542–8550
16. Han H, Jo S (2013) Supervised hierarchical Bayesian model-based electromyographic control and analysis. *IEEE J Biomed Health Inform* 18(4):1214–1224
17. He J, Zhang D, Sheng X, Li S, Zhu X (2014) Invariant surface EMG feature against varying contraction level for myoelectric control based on muscle coordination. *IEEE J Biomed Health Inform* 19(3):874–882
18. Ives JC, Wigglesworth JK (2003) Sampling rate effects on surface EMG timing and amplitude measures. *Clin Biomech* 18(6):543–552
19. Jung H, Ko C, Kim JS, Lee B, Lim D (2015) Alterations of relative muscle contribution induced by hemiplegia: straight and turning gaits. *Int J Precis Eng Manuf* 16(10):2219–2227
20. Khushaba RN, Kodagoda S, Takruri M, Dissanayake G (2012) Toward improved control of prosthetic fingers using surface electromyogram (EMG) signals. *Expert Syst Appl* 39(12):10731–10738
21. Kiguchi K, Hayashi Y (2012) An EMG-based control for an upper-limb power-assist exoskeleton robot. *IEEE Trans Syst Man Cybern Part B Cybern* 42(4):1064–1071
22. Kilbreath SL, Gandevia SC (1994) Limited independent flexion of the thumb and fingers in human subjects. *J Physiol* 479(Pt 3):487–497
23. Lee SW, Wilson KM, Lock BA, Kamper DG (2011) Subject-specific myoelectric pattern classification of functional hand movements for stroke survivors. *IEEE Trans Neural Syst Rehabil Eng* 19(5):558–566
24. Lee S, Kim H, Jeong H, Kim J (2015) Analysis of musculoskeletal system of human during lifting task with arm using electromyography. *Int J Precis Eng Manuf* 16(2):393–398
25. Matrone GC, Cipriani C, Carrozza MC, Magenes G (2012) Real-time myoelectric control of a multi-fingered hand prosthesis using principal components analysis. *J Neuroeng Rehabil* 9(1):40
26. Micera S, Carpaneto J, Raspopovic S (2010) Control of hand prostheses using peripheral information. *IEEE Rev Biomed Eng* 3:48–68
27. Momen K, Krishnan S, Chau T (2007) Real-time classification of forearm electromyographic signals corresponding to user-selected intentional movements for multifunction prosthesis control. *IEEE Trans Neural Syst Rehabil Eng* 15(4):535–542
28. Naik G, Nguyen H (2015) Non negative matrix factorization for the identification of EMG finger movements: evaluation using matrix analysis. *IEEE J Biomed Health Inform* 19(2):478–485
29. Naik GR, Baker KG, Nguyen HT (2014) Dependency independence measure for posterior and anterior EMG sensors used in simple and complex finger flexion movements: evaluation using SDICA. *IEEE J Biomed Health Inform* 19(5):1689–1696
30. Naik GR, Member S, Al-Timemy A, Nguyen HT (2016) Transradial amputee gesture classification using an optimal number of sEMG sensors: an approach using ICA clustering. *IEEE Trans Neural Syst Rehabil Eng* 24(8):837–846
31. Oskoei MA, Hu H (2007) Myoelectric control systems—a survey. *Biomed Signal Process Control* 2(4):275–294
32. Ouyang G, Zhu X, Ju Z, Liu H (2014) Dynamical characteristics of surface EMG signals of hand grasps via recurrence plot. *IEEE J Biomed Health Inform* 18(1):257–265
33. Scheme E, Englehart K (2011) Electromyogram pattern recognition for control of powered upper-limb prostheses: state of the art and challenges for clinical use. *J Rehabil Res Dev* 48(6):643–659
34. Scheme E, Lock B, Hargrove L, Hill W, Kuraganti U, Englehart K (2013) Motion normalized proportional control for improved pattern recognition based myoelectric control. *IEEE Trans Neural Syst Rehabil Eng* 22(1):149–157
35. Shi J, Cai Y, Zhu J, Zhong J, Wang F (2013) SEMG-based hand motion recognition using cumulative residual entropy and extreme learning machine. *Med Biol Eng Comput* 51(4):417–427
36. Tenore FVG, Ramos A, Fahmy A, Acharya S, Etienne-Cummings R, Thakor NV (2009) Decoding of individuated finger movements using surface electromyography. *IEEE Trans Biomed Eng* 56(5):1427–1434
37. Wang G, Ren D (2013) Classification of surface electromyographic signals by means of multifractal singularity spectrum. *Med Biol Eng Comput* 51(3):277–284
38. Young AJ, Hargrove LJ, Kuiken TA (2012) Improving myoelectric pattern recognition robustness to electrode shift by changing interelectrode distance and electrode configuration. *IEEE Trans Biomed Eng* 59(3):645–652
39. Young AJ, Smith LH, Rouse EJ, Hargrove LJ (2013) Classification of simultaneous movements using surface EMG pattern recognition. *IEEE Trans Biomed Eng* 60(5):1250–1258
40. Yu H-L, Chase RA, Strauch B (2003) *Atlas of hand anatomy and clinical implications*. Mosby, St. Louis



**Youngjin Na** received the M.S. and Ph.D. degree from the Department of Mechanical Engineering, Korea Advanced Institute of Science and Technology (KAIST), Daejeon, Republic of Korea, in 2011 and 2016, respectively. He is currently a Postdoctoral Researcher, Department of Mechanical Engineering, KAIST. His current research interests include biomedical signal processing and surface electromyography (sEMG)-based physical human–robot interactions.



**Sangjoon J. Kim** received his B.S. degree from the Department of Electrical and Computer Engineering from University of Wisconsin – Madison, in 2012. He has received his M.S. degree in Mechanical Engineering from Korea Advanced Institute of Science and Technology (KAIST), Daejeon, Republic of Korea, in 2014. Since 2014, he has been working towards his Ph.D. degree at KAIST. His research interests include wearable robotics, physical human

robot interaction, MR-compatible robots and rehabilitation robotics.



**Jung Kim** received the Ph.D. degree from the Department of Mechanical Engineering, Massachusetts Institute of Technology (MIT), Cambridge, MA, USA, in 2004. He is currently a Professor with the Department of Mechanical Engineering, Korea Advanced Institute of Science and Technology (KAIST), Daejeon, Republic of Korea. His current research interests include haptics, biosignal analysis for healthcare, and physical human–robot interactions.



**Sungho Jo** received the B.S. degree from the School of Mechanical and Aerospace Engineering, Seoul National University, Korea, in 1999, and the M.S. degree in Mechanical Engineering and the Ph.D. degree in Electrical Engineering and Computer Science both from the Massachusetts Institute of Technology (MIT), Cambridge, MA, USA, in 2001 and 2006, respectively. While pursuing the Ph.D. degree, he was with the Computer Science and Artificial Intel-

ligence Laboratory and the Laboratory for Information Decision and Systems. From 2006 to 2007, he was a Postdoctoral Researcher with the MIT Media Lab. Since December 2007, he has been with School of Computing, Korea Advanced Institute of Science and Technology (KAIST), Daejeon, Republic of Korea, where he is currently an Associate Professor. His research interests include brain–machine interface, muscle–computer interface, and wearable computing.